Electronic Supplementary Material (ESI) for RSC Advances.

Enhancement of air-stability, π-stacking ability and charge transport properties of fluoroalkyl side chain engineered Naphthalene tetracarboxylic diimide compounds

Gautomi Gogoi[a,c], Labanya Bhattacharya[b], Smruti R Sahoo[b], Sridhar Sahu[b], Neelotpal Sen Sarma[a], Sagar Sharma[d*]

a Advanced Materials Laboratory, Physical Sciences Division, Institute of Advanced Study in Science and Technology, Vigyan Path, Paschim Boragaon, Guwahati-781035, Assam, India, Tel: +91-361-2270095

b High Performance Computing Lab, Department of Physics, Indian Institute of Technology (Indian School of Mines), Dhanbad, Jharkhand-826004, India

c Cotton University, College Hostel Road, Pan Bazaar, Guwahati-781001, Assam, India

d Department of Chemistry, School of Fundamental and Applied Sciences, Assam Don Bosco University, Tapesia Gardens, Guwahati-782402, Assam, India

1a	1b	1c	1d	
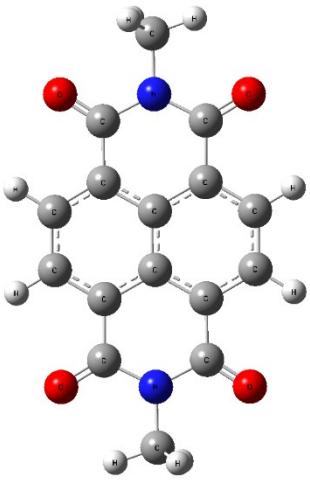	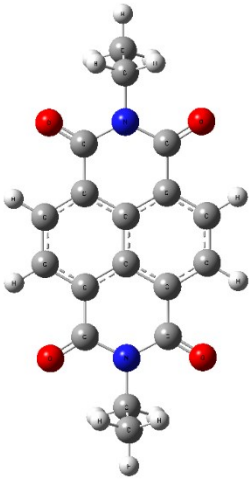	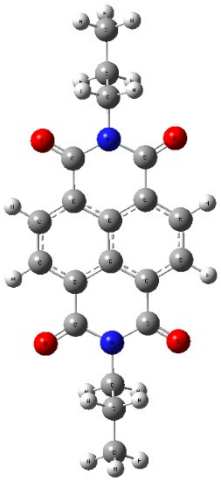	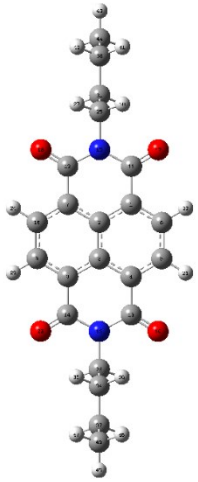	
2a	2b	2c	2d	2e
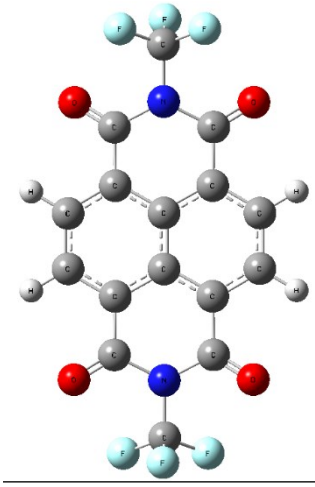	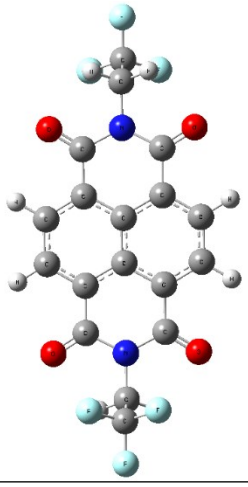	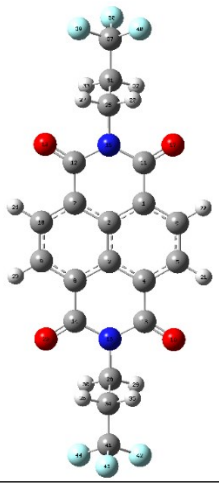	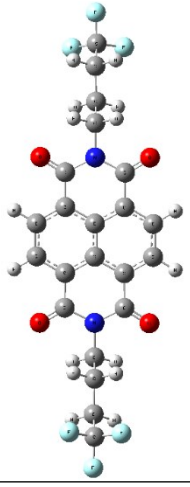	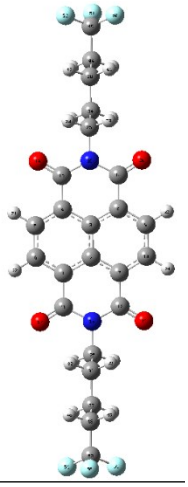
3a	3b	3c	3d	3e
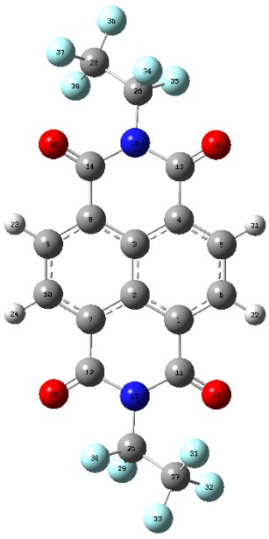	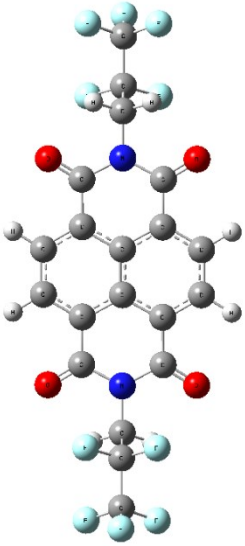	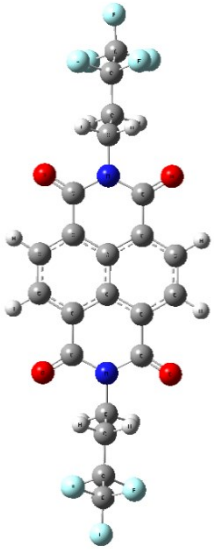	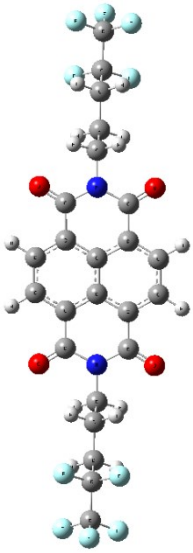	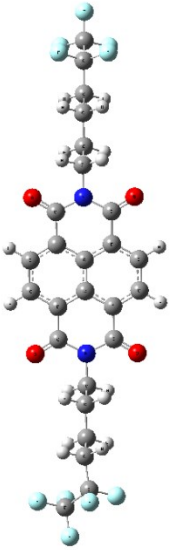
4a	4b	4c	4d	4e

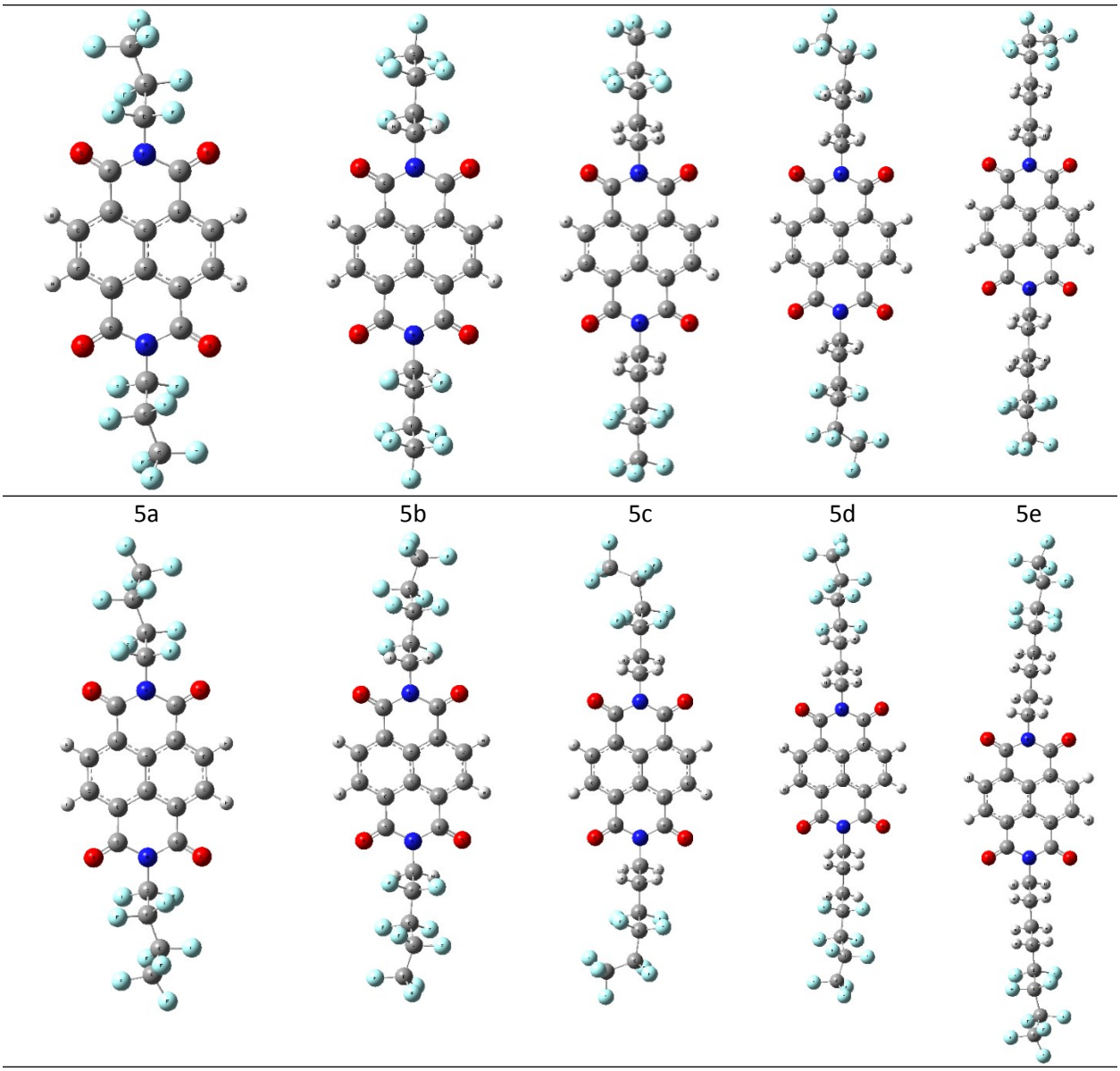

Fig. S1 Optimized geometries of the studied compounds

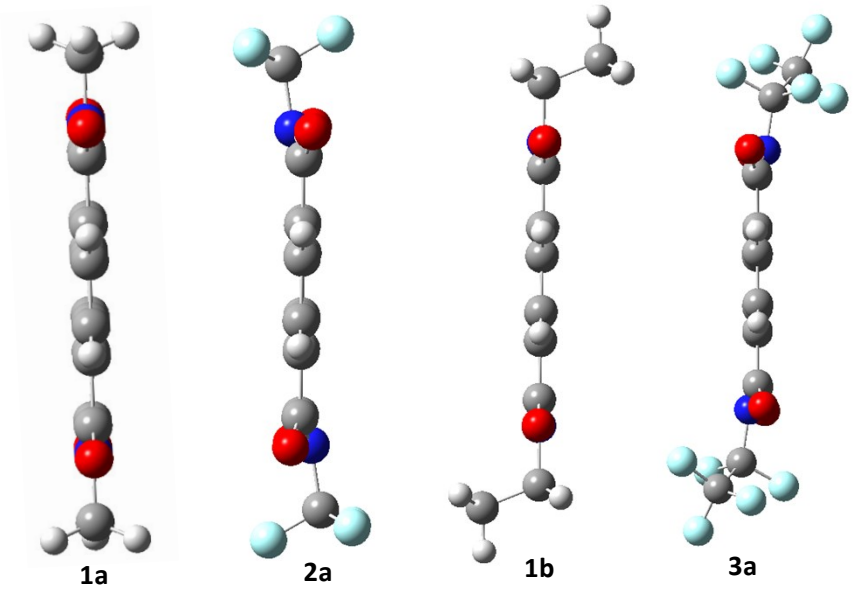

Fig. S2 Side view of four compounds

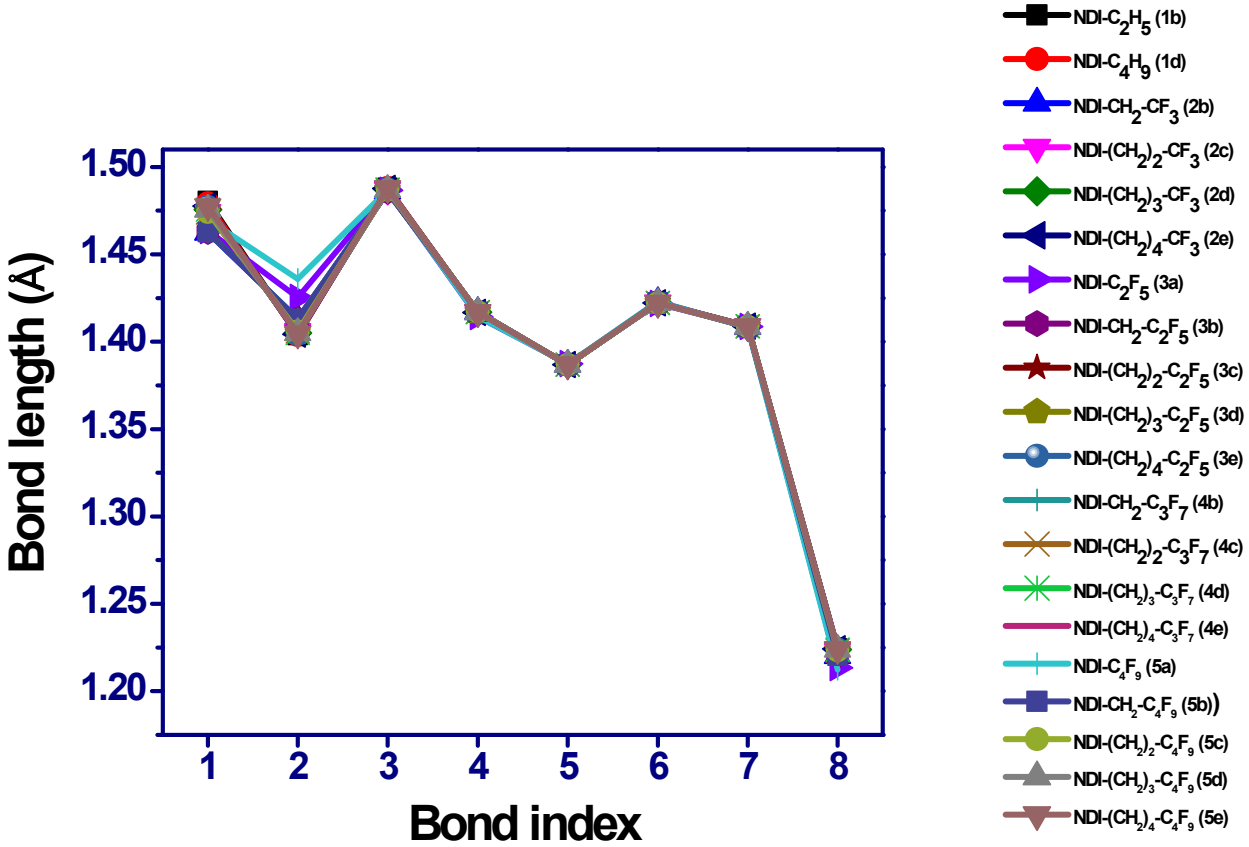

Fig. S3: Bond index of 20 compounds along the molecular backbone

Compound	HOMO	LUMO
1a	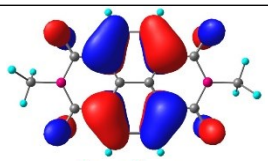	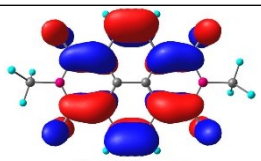
1b	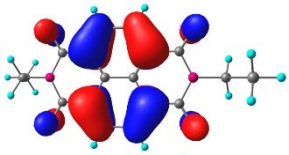	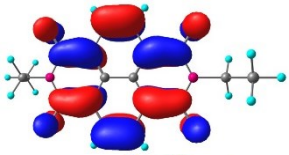
1c	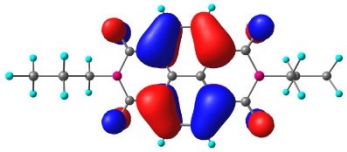	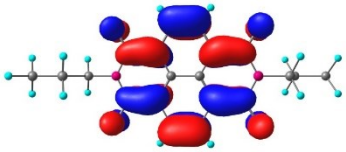
1d	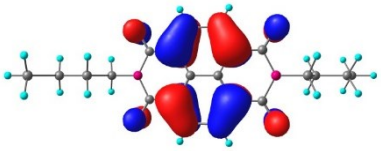	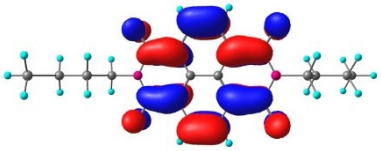
2a	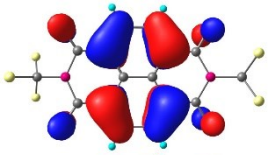	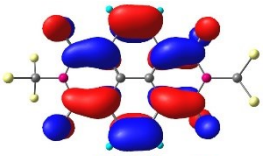
2b	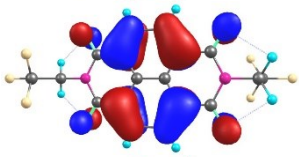	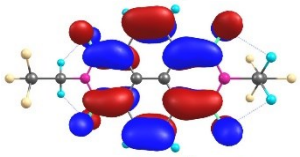
2c	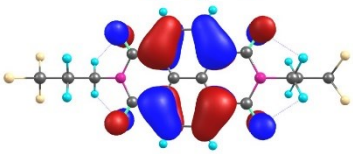	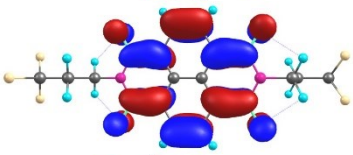
2d	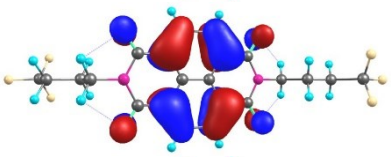	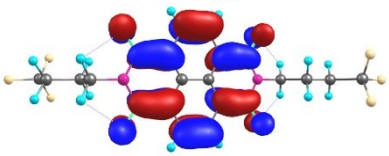
2e	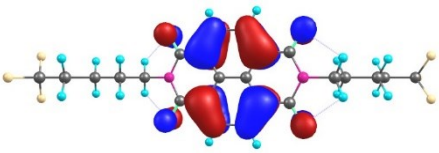	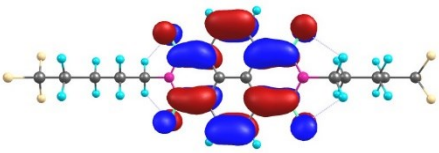
3a	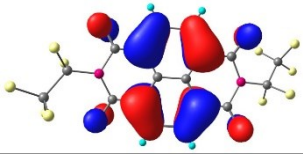	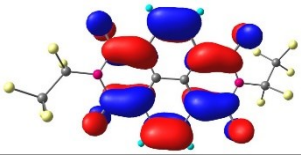

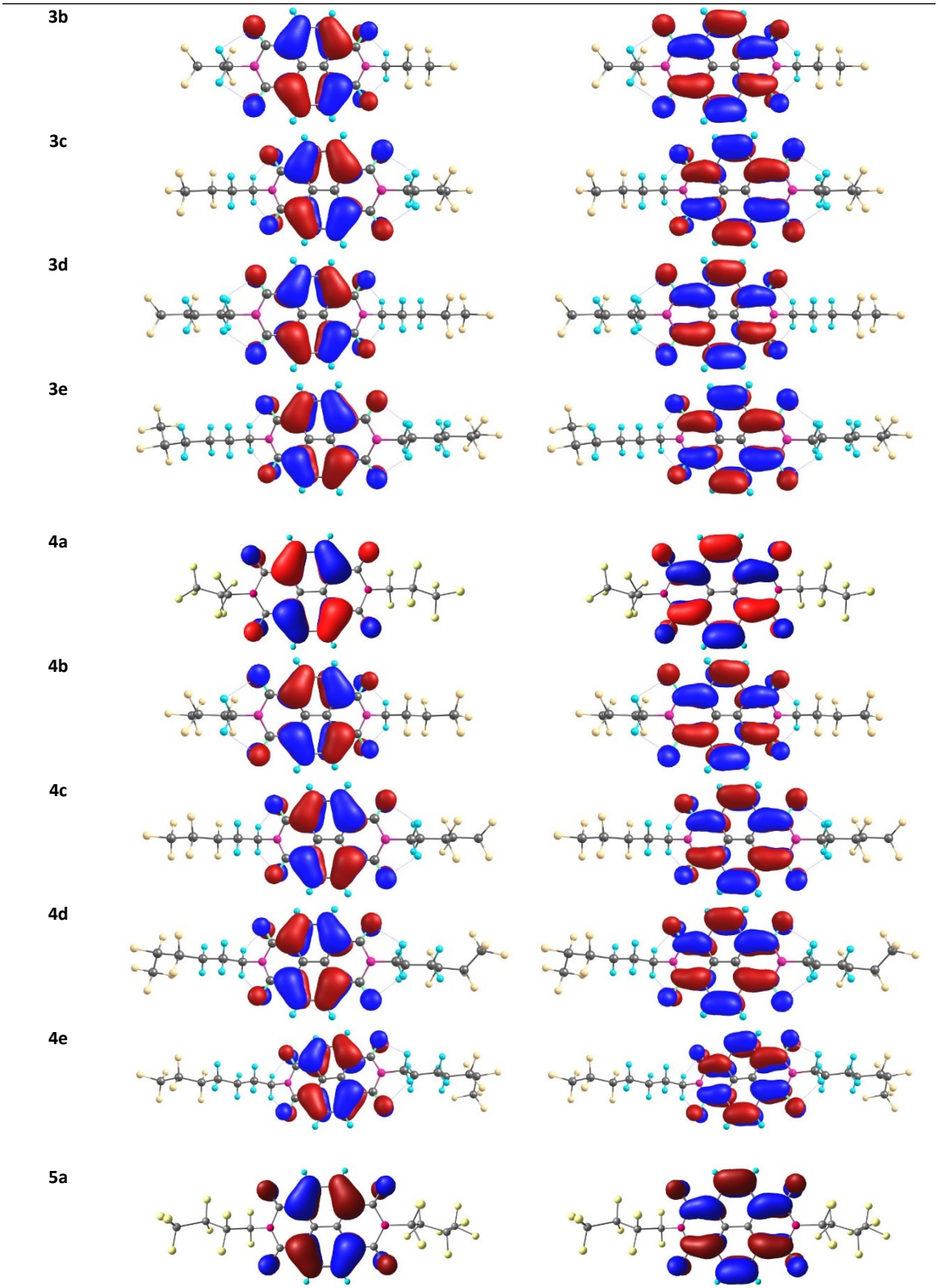
3b
3c
3d
3e
4a
4b
4c
4d
4e
5a

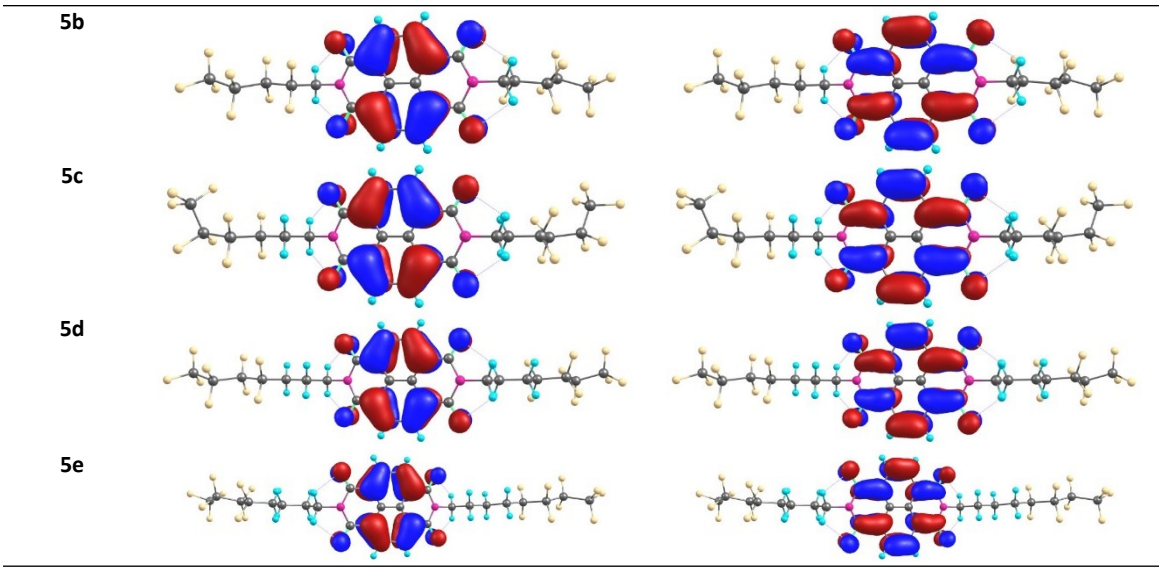

Fig. S4 Frontier molecular orbital plot of NDI-compounds

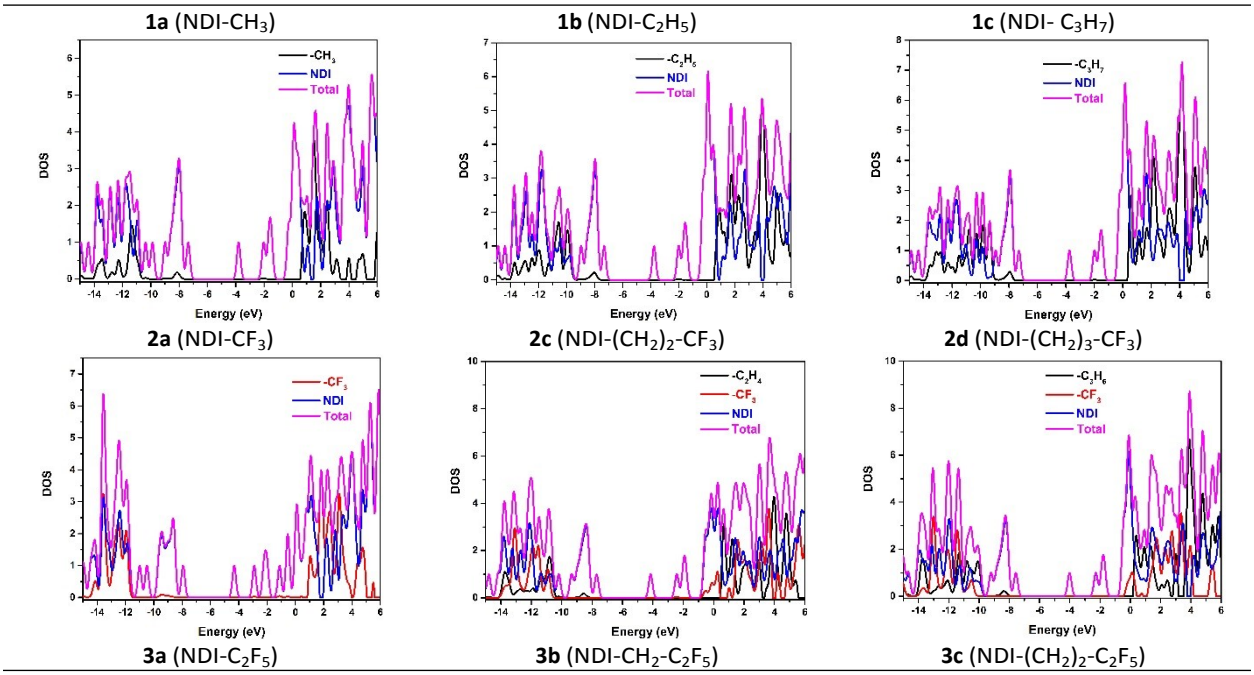

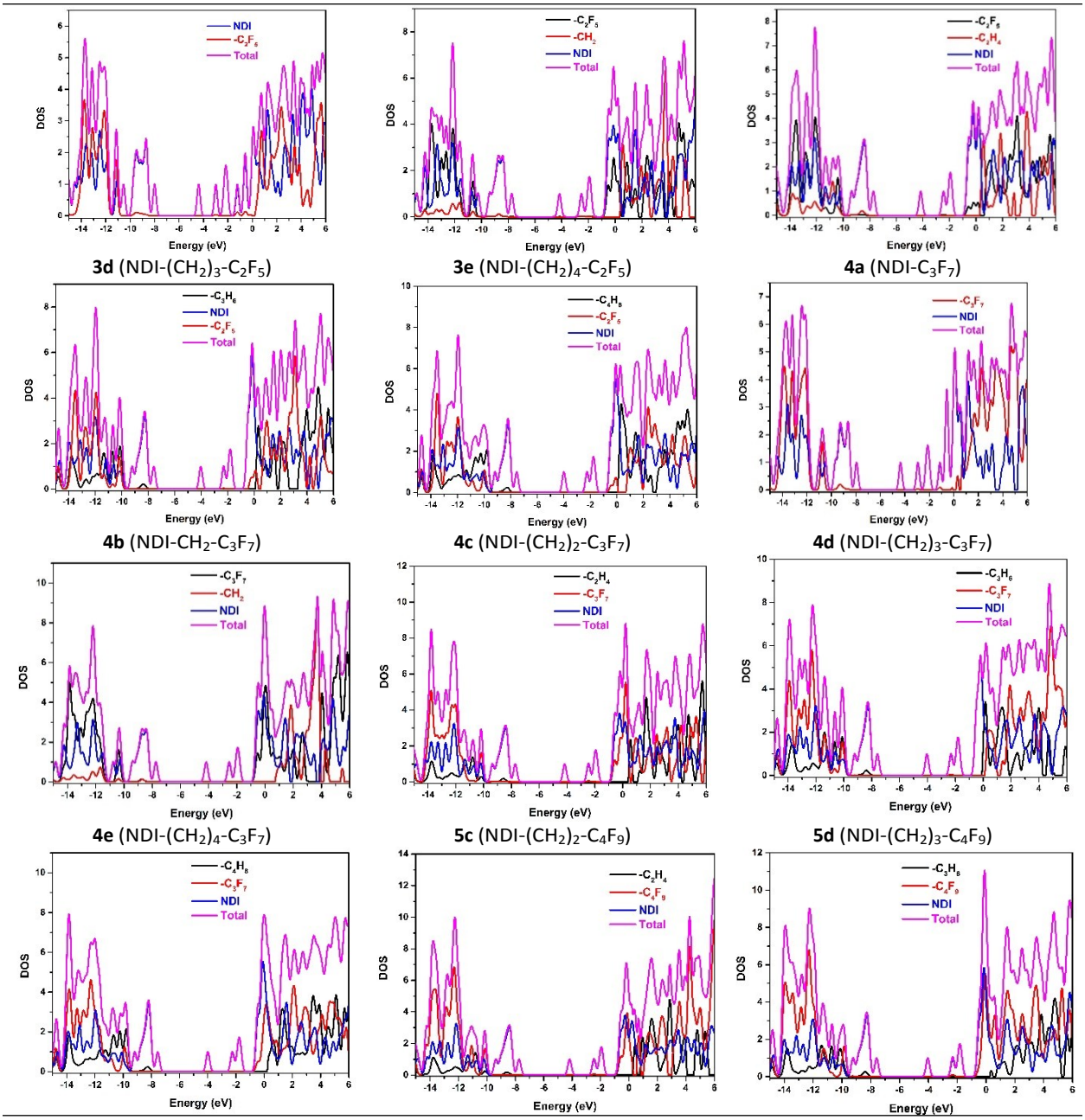

3d (NDI-$(CH_2)_3$-C_2F_5) **3e** (NDI-$(CH_2)_4$-C_2F_5) **4a** (NDI-C_3F_7)

4b (NDI-CH_2-C_3F_7) **4c** (NDI-$(CH_2)_2$-C_3F_7) **4d** (NDI-$(CH_2)_3$-C_3F_7)

4e (NDI-$(CH_2)_4$-C_3F_7) **5c** (NDI-$(CH_2)_2$-C_4F_9) **5d** (NDI-$(CH_2)_3$-C_4F_9)

Fig. S5 Density of states of NDI-compounds

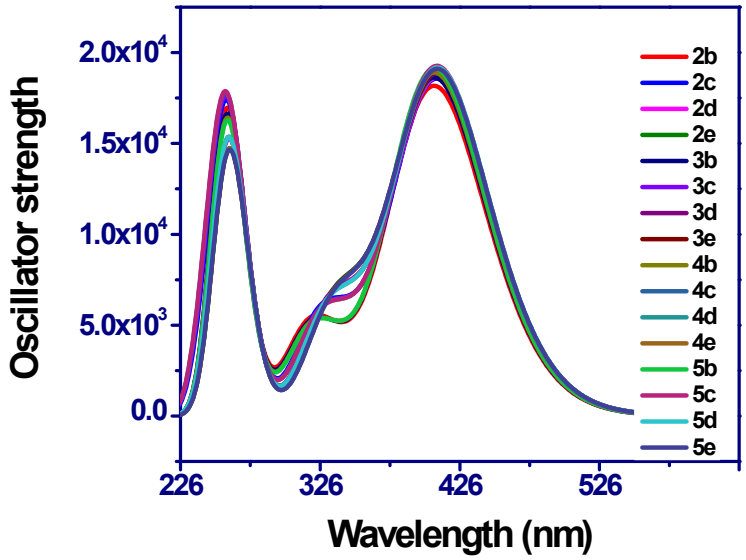

Fig. S6 Simulated absorption spectra of NDI-compounds at B3LYP/6-31+G(d,p) level in dicholoromethane solvent

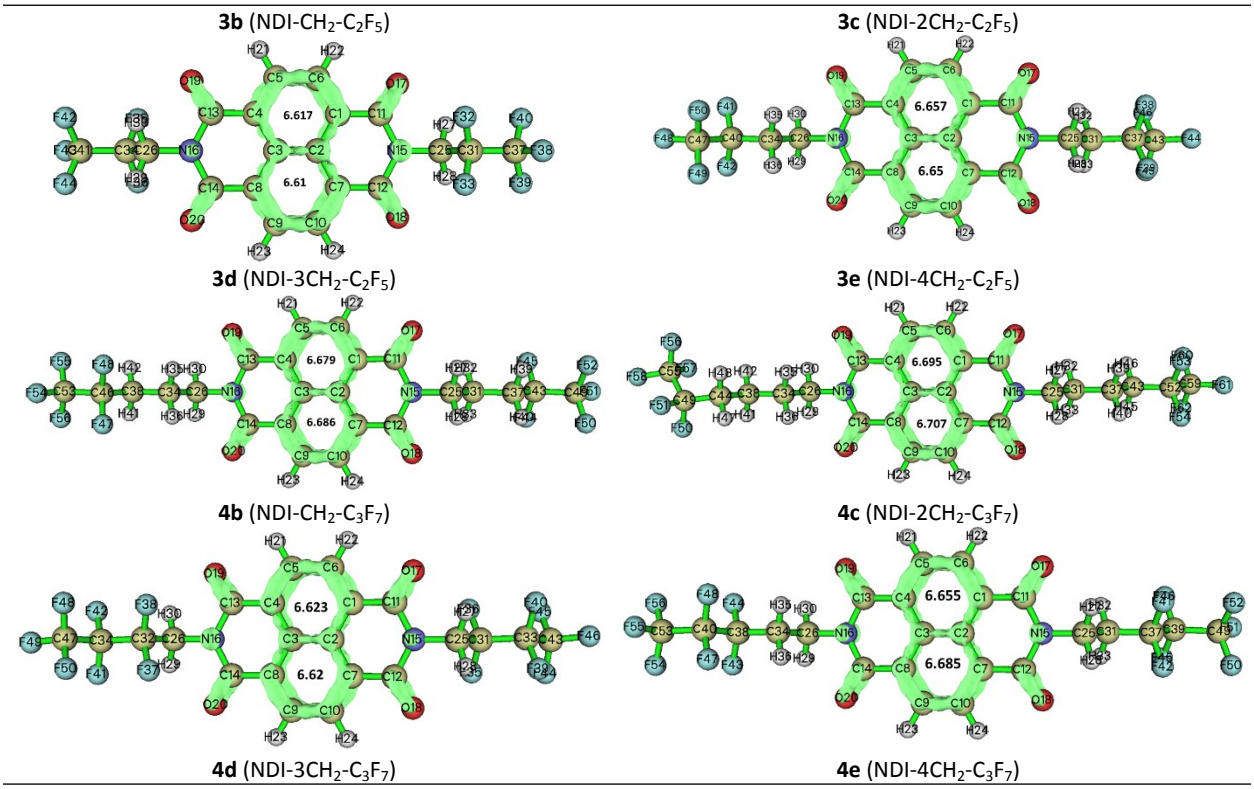

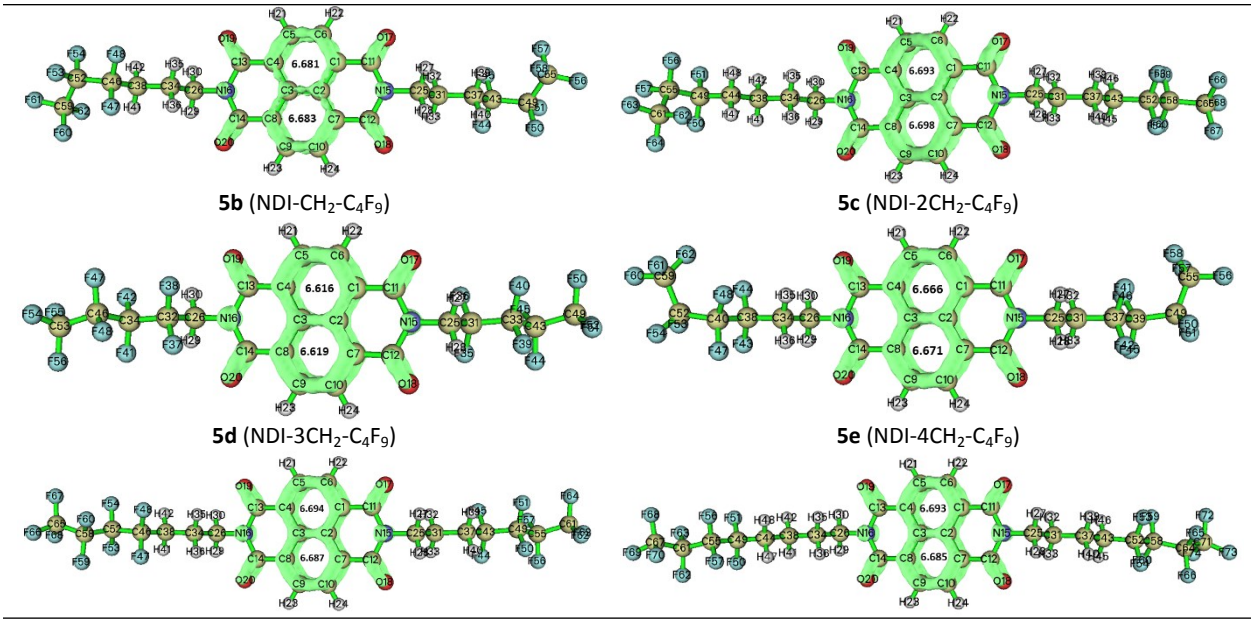

5b (NDI-CH_2-C_4F_9) **5c** (NDI-$2CH_2$-C_4F_9)

5d (NDI-$3CH_2$-C_4F_9) **5e** (NDI-$4CH_2$-C_4F_9)

Fig. S7 Localized orbital locator surface along with the LOLIPOP value for the studied compounds

Table S1 Bond index of the studied compounds along with the earlier reported crystal structure of six compounds with their references

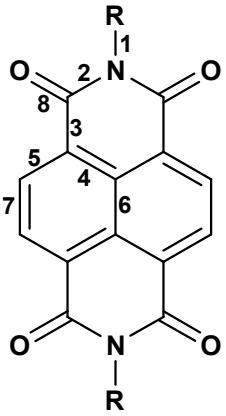

Bond index	**1a**
1	1.471[a] (1.475)[1]
2	1.405[a] (1.388)[1]
3	1.489[a] (1.483)[1]
4	1.417[a] (1.406)[1]
5	1.387[a] (1.375)[1]
6	1.422[a] (1.415)[1]
7	1.409[a] (1.398)[1]

8	$1.224^{a}\ (1.213)^{1}$

a : obtained at B3LYP/6-31+G(d,p) level of theory

Bond index	**1b**
1	$1.481^{a}\ (1.477)^{2}\ (1.474)^{3}$
2	$1.404^{a}\ (1.394)^{2}\ (1.387)^{3}$
3	$1.488^{a}\ (1.476)^{2}\ (1.473)^{3}$
4	$1.416^{a}\ (1.410)^{2}\ (1.397)^{3}$
5	$1.387^{a}\ (1.375)^{2}\ (1.373)^{3}$
6	$1.422^{a}\ (1.405)^{2}\ (1.404)^{3}$
7	$1.409^{a}\ (1.401)^{2}\ (1.396)^{3}$
8	$1.224^{a}\ (1.215)^{2}\ (1.210)^{3}$

a : obtained at B3LYP/6-31+G(d,p) level of theory

Bond index	**1c**
1	$1.479^{a}\ (1.479)^{4}\ (1.479)^{1}$
2	$1.404^{a}\ (1.397)^{4}\ (1.398)^{1}$
3	$1.488^{a}\ (1.487)^{4}\ (1.486)^{1}$
4	$1.416^{a}\ (1.417)^{4}\ (1.411)^{1}$
5	$1.387^{a}\ (1.377)^{4}\ (1.376)^{1}$
6	$1.422^{a}\ (1.413)^{4}\ (1.413)^{1}$
7	$1.409^{a}\ (1.402)^{4}\ (1.404)^{1}$
8	$1.224^{a}\ (1.216)^{4}\ (1.211)^{1}$

a : obtained at B3LYP/6-31+G(d,p) level of theory

Bond index	**1d**
1	$1.479^{a}\ (1.486)^{5}$
2	$1.404^{a}\ (1.401)^{5}$
3	$1.488^{a}\ (1.481)^{5}$
4	$1.416^{a}\ (1.411)^{5}$
5	$1.387^{a}\ (1.381)^{5}$
6	$1.423^{a}\ (1.415)^{5}$
7	$1.409^{a}\ (1.402)^{5}$
8	$1.224^{a}\ (1.217)^{5}$

a : obtained at B3LYP/6-31+G(d,p) level of theory

Bond index	**4b**
1	1.463[a] (1.468)[6] (1.460)[7]
2	1.413[a] (1.398)[6] (1.394)[7]
3	1.486[a] (1.477)[6] (1.486)[7]
4	1.417[a] (1.390)[6] (1.418)[7]
5	1.387[a] (1.380)[6] (1.369)[7]
6	1.423[a] (1.434)[6] (1.414)[7]
7	1.409[a] (1.402)[6] (1.400)[7]
8	1.220[a] (1.213)[6] (1.221)[7]

a: obtained at B3LYP/6-31+G(d,p) level of theory

Table S2 Dihedrel angle of the studied compounds along with the earlier reported crystal structure of 6 compounds

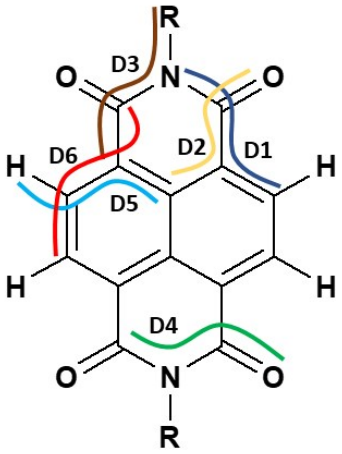

Dihedrel angle	1a (in °)
D1	-179.9[a] (-176.6)[1]
D2	-179.9[a] (-175.3)[1]
D3	-179.9[a] (-179.2)[1]
D4	-179.9[a] (179.4)[1]
D5	-179.9[a] (-178.9)[1]
D6	-180.0[a] (-177.9)[1]

a: obtained at B3LYP/6-31+G(d,p) level of theory

Dihedrel angle	1b (in °)
D1	179.1[a] (177.2)[2] (176.9)[3]
D2	179.3[a] (177.0)[2](177.1)[3]
D3	179.4[a] (177.3)[2] (177.1)[3]
D4	178.2[a] (-177.5)[2] (-177.5)[3]
D5	179.9[a] (178.9)[2] (178.9)[3]
D6	179.9[a] (177.7)[2] (178.0)[3]

a: obtained at B3LYP/6-31+G(d,p) level of theory

Dihedrel angle	1c (in °)
D1	179.1[a] (179.2)[1]
D2	179.4[a] (-179.5)[1]
D3	179.3[a] (179.3)[1]
D4	178.3[a] (178.2)[1]
D5	179.9[a] (-179.8)[1]
D6	179.9[a] (-179.4)[1]

a : obtained at B3LYP/6-31+G(d,p) level of theory

Dihedrel angle	1d (in °)
D1	179.2[a] (-177.4)[5]
D2	179.3[a] (-175.4)[5]
D3	179.5[a] (177.1)[5]
D4	178.4[a] (-179.4)[5]
D5	179.9[a] (-179.4)[5]
D6	179.9[a] (-179.3)[5]

a : obtained at B3LYP/6-31+G(d,p) level of theory

Dihedrel angle	4b (in °)
D1	175.7[a] (173.7)[6] (-174.4)[7]
D2	175.8[a] (175.3)[6] (-172.4)[7]
D3	178.4[a] (174.4)[6] (178.6)[7]
D4	170.9[a] (171.2)[6] (-173.4)[7]
D5	179.9[a] (179.4)[6] (-178.6)[7]
D6	179.6[a] (178.6)[6] (-178.0)[7]

a : obtained at B3LYP/6-31+G(d,p) level of theory

Table S3 HOMO, LUMO and band gap values in eV for all the studied compounds at B3LYP/6-31+G(d,p) level

Compound	HOMO	LUMO	Band gap
1a	-7.35	-3.78	3.57
1b	-7.30	-3.74	3.56
1c	-7.29	-3.73	3.56
1d	-7.28	-3.72	3.56
2a	-7.92	-4.31	3.61
2b	-7.71	-4.14	3.57
2c	-7.69	-4.13	3.56
2d	-7.56	-4.00	3.56
2e	-7.52	-3.96	3.56
3a	-7.92	-4.33	3.59
3b	-7.72	-4.15	3.57
3c	-7.71	-4.15	3.56
3d	-7.57	-4.01	3.56
3e	-7.53	-3.97	3.56
4a	-7.93	-4.34	3.59
4b	-7.73 (-6.84)[8]	-4.16 (-3.72)[8]	3.57 (3.12)[8]
4c	-7.71	-4.15	3.56
4d	-7.58	-4.02	3.56
4e	-7.53	-3.98	3.56
5a	-7.94	-4.34	3.59
5b	-7.74	-4.16	3.57
5c	-7.72	-4.16	3.56
5d	-7.58	-4.03	3.56
5e	-7.54	-3.98	3.56

Table S4 Computed electronic transition energy (E), absorption wavelength (λ), oscillator strength (*f*) and transition and major composition for dominant excitations in dichloromethane solvent b3lyp/6-31+G(d,p) level

Compound	State	E (eV)	λ (nm)	f	Major Configuration
2b	S1	3.2197	385	0.4107	HOMO->LUMO (98%)
	S15	5.3065	234	0.4167	HOMO->L+3 (83%)
2c	S1	3.2115	386	0.4294	HOMO->LUMO (99%)
	S14	5.2814	235	0.3775	HOMO->L+3 (82%)
2d	S1	3.2105	386	0.4363	HOMO->LUMO (99%)
	S14	5.2675	235	0.353	HOMO->L+2 (81%)
2e	S1	3.2108	386	0.4409	HOMO->LUMO (99%)
	S15	5.2582	236	0.3371	HOMO->L+2 (80%)
3b	S1	3.2197	385	0.4221	HOMO->LUMO (98%)
	S15	5.3053	234	0.4081	HOMO->L+3 (83%)
3c	S1	3.2110	386	0.437	HOMO->LUMO (99%)
	S14	5.2815	235	0.3726	HOMO->L+3 (82%)
3d	S1	3.2101	386	0.4423	HOMO->LUMO (99%)
	S14	5.2677	235	0.3516	HOMO->L+2 (81%)
3e	S1	3.2104	386	0.4456	HOMO->LUMO (99%)
	S14	5.2584	236	0.3358	HOMO->L+2 (80%)
4b	S1	3.2194	385	0.4295	HOMO->LUMO (98%)
	S15	5.3046	234	0.402	HOMO->L+3 (83%)
4c	S1	3.2106	386	0.4433	HOMO->LUMO (99%)
	S14	5.2814	235	0.3705	HOMO->L+3 (82%)
4d	S1	3.2101	386	0.4472	HOMO->LUMO (99%)
	S14	5.2676	235	0.3508	HOMO->L+2 (81%)
4e	S1	3.2103	386	0.4478	HOMO->LUMO (99%)
	S15	5.2579	236	0.3161	HOMO->L+2 (76%)

5b	S1	3.2189	385	0.4353	HOMO->LUMO (98%)
	S15	5.3039	234	0.3982	HOMO->L+3 (83%)
5c	S1	3.2104	386	0.4472	HOMO->LUMO (99%)
	S15	5.2811	235	0.3673	HOMO->L+3 (81%)
5d	S1	3.2096	386	0.4497	HOMO->LUMO (99%)
	S14	5.2674	235	0.3481	HOMO->L+2 (81%)
5e	S1	3.2099	386	0.45	HOMO->LUMO (99%)
	S15	5.2573	236	0.3102	HOMO->L+2 (75%)

Table S5 Computed electronic transition energy (E), absorption wavelength (λ), oscillator strength (*f*) and transition and major composition for dominant excitations in dichloromethane solvent at cam-b3lyp/6-31+G(d,p) level

Compound	State	E (eV)	λ (nm)	f	Major Configuration
1a (NDI-CH_3)	S1	3.5491	349	0.4877	HOMO->LUMO (98%)
	S12	5.6673	219	0.8051	HOMO->L+2 (79%)
1b (NDI-C_2H_5)	S1	3.5437	350	0.5063	HOMO->LUMO (98%)
	S12	5.6577	219	0.7772	HOMO->L+2 (79%)
1c (NDI- C_3H_7)	S1	3.5423	350	0.5227	HOMO->LUMO (98%)
	S12	5.6528	219	0.7535	HOMO->L+2 (79%)
	S19	6.4413	192	0.3441	H-2->L+1 (39%)
1d (NDI-C_4H_9)	S1	3.5422	350	0.5297	HOMO->LUMO (98%)
	S12	5.6517	219	0.7424	HOMO->L+2 (80%)
	S19	6.4400	193	0.3762	H-2->L+1 (39%)
2a (NDI-CF_3)	S1	3.5947	345	0.477	HOMO->LUMO (98%)
	S12	5.8073	213	0.9293	HOMO->L+2 (46%)
2b (NDI-CH_2-CF_3)	S1	3.5547	349	0.507	HOMO->LUMO (98%)
	S12	5.7013	217	0.832	HOMO->L+2 (76%)
2c (NDI-$(CH_2)_2$-CF_3)	S1	3.5431	350	0.5240	HOMO->LUMO (98%)
	S12	5.6790	218	0.7959	HOMO->L+2 (78%)
2d (NDI-$(CH_2)_3$-CF_3)	S1	3.5413	350	0.5308	HOMO->LUMO (98%)
	S12	5.6659	219	0.7678	HOMO->L+2 (79%)
2e (NDI-$(CH_2)_4$-CF_3)	S1	3.5417	350	0.5359	HOMO->LUMO (98%)
	S12	5.6581	219	0.7515	HOMO->L+2 (79%)
	S19	6.4511	192	0.3067	H-2->L+1 (36%)

3a (NDI-C_2F_5)	S1	3.5746	347	0.4994	HOMO->LUMO (98%)
	S12	5.7767	215	0.9017	HOMO->L+2 (54%)
3b (NDI-CH_2-C_2F_5)	S1	3.5552	349	0.5215	HOMO->LUMO (98%)
	S12	5.6996	218	0.8148	HOMO->L+2 (76%)
3c (NDI-$(CH_2)_2$-C_2F_5)	S1	3.5428	350	0.533	HOMO->LUMO (98%)
	S12	5.6790	218	0.7857	HOMO->L+2 (78%)
3d (NDI-$(CH_2)_3$-C_2F_5)	S1	3.5410	350	0.5378	HOMO->LUMO (98%)
	S12	5.6660	219	0.7639	HOMO->L+2 (79%)
3e (NDI-$(CH_2)_4$-C_2F_5)	S1	3.5413	350	0.5416	HOMO->LUMO (98%)
	S12	5.6582	219	0.7487	HOMO->L+2 (79%)
	S19	6.4511	192	0.3174	H-2->L+1 (36%)
4a (NDI-C_3F_7)	S1	3.5766	347	0.5154	HOMO->LUMO (98%)
	S12	5.7766	215	0.8832	HOMO->L+2 (54%)
4b (NDI-CH_2-C_3F_7)	S1	3.5548	349	0.5297	HOMO->LUMO (98%)
	S12	5.6986	218	0.8045	HOMO->L+2 (76%)
4c (NDI-$(CH_2)_2$-C_3F_7)	S1	3.5423	350	0.5402	HOMO->LUMO (98%)
	S12	5.6788	218	0.7804	HOMO->L+2 (78%)
4d (NDI-$(CH_2)_3$-C_3F_7)	S1	3.5410	350	0.5436	HOMO->LUMO (98%)
	S12	5.6661	219	0.7602	HOMO->L+2 (79%)
4e (NDI-$(CH_2)_4$-C_3F_7)	S1	3.5411	350	0.544	HOMO->LUMO (98%)
	S12	5.6578	219	0.7461	HOMO->L+2 (79%)
	S19	6.4485	192	0.3321	H-2->L+1 (37%)
5a (NDI-C_4F_9)	S1	3.5763	347	0.5257	HOMO->LUMO (98%)
	S12	5.7747	215	0.8722	HOMO->L+2 (54%)
5b (NDI-CH_2-C_4F_9)	S1	3.5542	349	0.5363	HOMO->LUMO (98%)
	S12	5.6981	218	0.7989	HOMO->L+2 (76%)
5c (NDI-$(CH_2)_2$-C_4F_9)	S1	3.5421	350	0.5449	HOMO->LUMO (98%)
	S12	5.6785	218	0.7771	HOMO->L+2 (78%)
5d (NDI-$(CH_2)_3$-C_4F_9)	S1	3.5405	350	0.546	HOMO->LUMO (98%)
	S12	5.6658	219	0.757	HOMO->L+2 (79%)
5e (NDI-$(CH_2)_4$-C_4F_9)	S1	3.5407	350	0.5463	HOMO->LUMO (98%)
	S12	5.6577	219	0.7432	HOMO->L+2 (79%)
	S19	6.4472	192	0.3406	H-2->L+1 (37%)

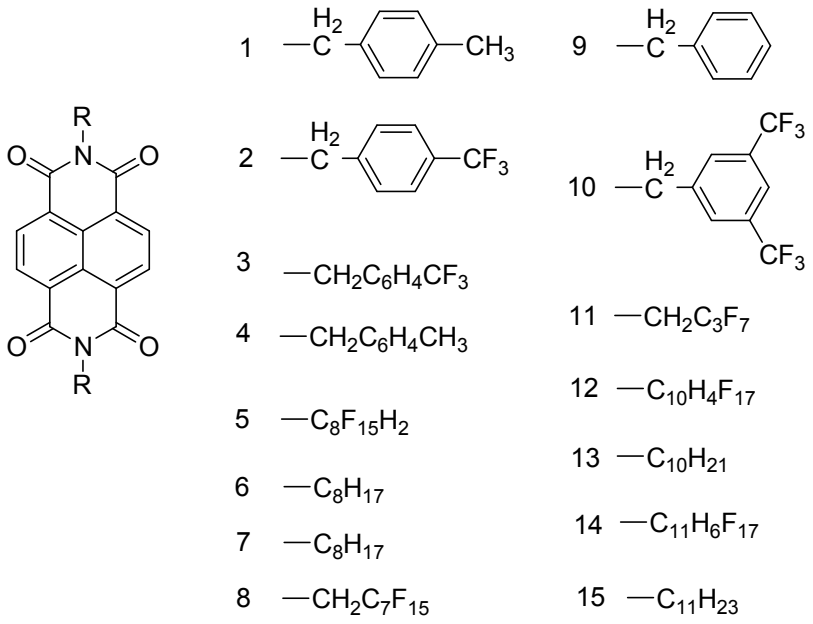

Figure. S8 Some naphthalene tetracarboxylic diimide (NDI) compounds reported earlier

Table S6 Mobility and LUMO energy level of NDI compounds in air reported earlier

Compound	Mobility in air (cm^2/Vs)	LUMO energy (eV)	Reference
1	No mobility		[9]
2	0.12		[9]
3	0.01		[10]
4	No mobility		[10]
5	0.01		[10]
6	10^{-6}		[10]
7	No mobility		[11]
8	0.1		[11]
9	$1.2x10^{-3}$		[12]
10	$1.2x10^{-3}$		[12]
11	0.26±0.02	-3.72	[13]
12	0.029	-3.77	[14]
13	0.32	-3.64	[15]
14	0.38	-3.71	[15]
15	0.15	-3.64	[15]

The side chain engineering of rylene diimides (naphthalene diimide, NDI and perylene diimide, PDI) with fluoro groups can significantly increase the stability of the compound as self-segregation of fluoro groups occur followed by a densely packed structure. The movement of oxygen and moisture can be hindered through this densely packed structure[15,16]. Byung Jun Jung *et al* reported a series of naphthalene tetracarboxylic diimide based compounds with increasing fluoro groups in the side chain[17] as shown on the following Figure S9.

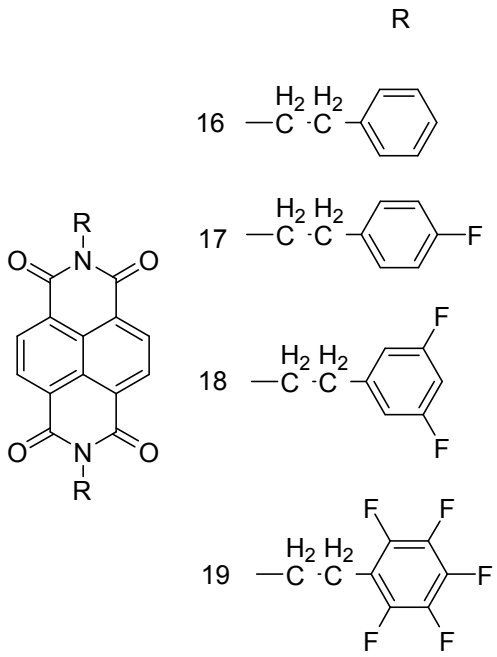

Fig. S9 A series of naphthalene tetracarboxylic diimide (NDI) compounds with increasing fluoro groups

In their work, the highest mobility observed for compound 19 is as high as 0.064±0.017 cm^2/Vs among the reported four compounds (**16**, **17**, **18**, **19**) due to the effect of larger number of fluoro groups. Brooks A. Jones *et al* have reported the air stability of NDI compound with fluoroalkyl side chain engineering as shown on the following Figure S10 with electron mobility of 0.1 cm^2/Vs[18] in air. Its N-alkyl derivative has no mobility due to its less densely packed structure and instability in air.

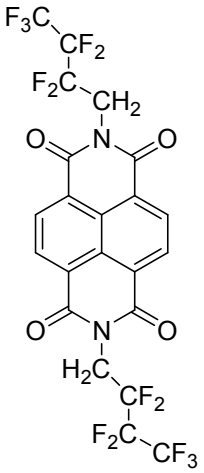

Fig. S10 NDI compound with fluoroalkyl side chain

Reference:

[1] G. R. Krishna, R. Devarapalli, G. Lal, and C. M. Reddy, Mechanically Flexible Organic Crystals Achieved by Introducing Weak Interactions in Structure: Supramolecular Shape Synthons, *J. Am. Chem. Soc*., 2016, **138**, 13561−13567.

[2] M. Pandeeswar, H. Khare, S. Ramakumar and T. Govindaraju, Biomimetic molecular organization of naphthalene diimide in the solid state: tunable (chiro-) optical, viscoelastic and nanoscale properties, *RSC Adv*., 2014, **4**, 20154–20163.

[3] R. Devarapalli, S. B. Kadambi, C. T. Chen, G. R.Krishna, B. R. Kammari, M. J. Buehler, U. Ramamurty and C. Malla Reddy, Remarkably Distinct Mechanical Flexibility in Three Structurally Similar Semiconducting Organic Crystals Studied by Nanoindentation and Molecular Dynamics, *Chem. Mater*. 2019, **31**, 1391−1402.

[4] X. Zhao, Y. Xiong, J. Ma, and Z. Yuan, Rylene and Rylene Diimides: Comparison of Theoretical and Experimental Results and Prediction for High-Rylene Derivatives, *J. Phys. Chem. A*, 2016, **120**, 7554−7560.

[5] P. M. Alvey, J. J. Reczek, V. Lynch and B. L. Iverson, A Systematic Study of Thermochromic Aromatic Donor-Acceptor Materials, *J. Org. Chem*., 2010, **75**, 7682–7690.

6 D. Shukla, M. Rajeswaran, W. G. Ahearn and D. M. Meyer, N,N-Bis(2,2,3,3,4,4,4 heptafluorobutyl)-naphthalene-1,4:5,8-tetracarboximide, *Acta Cryst*., 2008, **E64**, o2327.

[7] A. Lv, Y. Li, W. Yue, L. Jiang, H. Dong, G. Zhao, Q Meng, W. Jiang, Y. He, Z. Li, Z. Wang and W. Hu, High performance n-type single crystalline transistors of naphthalene bis(dicarboximide) and their anisotropic transport in crystals, *Chem. Commun*., 2012, **48**, 5154–5156.

8 J. H. Oh, S. L. Suraru, W. Y. Lee, M. Konemann, H. W. Hoffken, C. Roger, R. Schmidt, Y. Chung, W. C. Chen, F. Wurthner and Z. Bao, High-Performance Air-Stable n-Type Organic Transistors Based on Core-Chlorinated Naphthalene Tetracarboxylic Diimides, *Adv. Funct. Mater*., 2010, **20**, 2148–2156

[9] H. E. Katz, Theo Siegrist, J. Hendrik Schon, Christian Kloc, Bertram Batlogg, Andrew J. Lovinger, Jerainne Johnson, Solid-State Structural and Electrical Characterization of N-Benzyl and N-Alkyl Naphthalene 1,4,5,8-Tetracarboxylic Diimides, *Chem. Phys. Chem*. 2001, **2**, 167-172.

[10] H. E. Katz, Jerainne Johnson,† Andrew J. Lovinger, and Wenjie Li, Naphthalenetetracarboxylic Diimide-Based n-Channel Transistor Semiconductors: Structural Variation and Thiol-Enhanced Gold Contacts, J*. Am. Chem. Soc*. 2000, **122**, 7787-7792.

[11] H. E. Katz, A. J. Lovinger, J. Johnson, C. Kloc, T. Siegrist, W. Li, Y.-Y. Lin & A. Dodabalapur, A soluble and air-stable organic semiconductor with high electron mobility, *Nature*, 2000, **404**, 478-481.

[12] Y. L. Lee, Hui-Lin Hsu, Szu-Ying Chen, and Tri-Rung Yew, Solution-Processed Naphthalene Diimide Derivatives as n-Type Semiconductor Materials, *J. Phys. Chem. C*, 2008, **112***,* 1694-1699.

[13] J. H. Oh, Sabin–Lucian Suraru, Wen-Ya Lee, Martin Konemann, Hans Wolfgang Hoffken, Cornelia Roger, Rudiger Schmidt, Yoonyoung Chung, Wen-Chang Chen, Frank Wurthner, Zhenan Bao, High-Performance Air-Stable n-Type OrganicTransistors Based on Core-Chlorinated Naphthalene Tetracarboxylic Diimides, *Adv. Funct. Mater*. 2010, **20**, 2148–2156.

[14] B. J. Jung, Kyusang Lee, Jia Sun, Andreas G. Andreou, Howard E. Katz, Air-Operable, High-Mobility Organic Transistors with Semifluorinated Side Chains and Unsubstituted Naphthalenetetracarboxylic Diimide Cores: High Mobility and Environmental and Bias Stress Stability from the Perfluorooctylpropyl Side Chain, *Adv. Funct. Mater*. 2010, **20**, 2930–2944.

[15] R. Devarapalli, S. B. Kadambi, C. T. Chen, G. R.Krishna, B. R. Kammari, M. J. Buehler, U. Ramamurty and C. Malla Reddy, Remarkably Distinct Mechanical Flexibility in Three Structurally Similar Semiconducting Organic Crystals Studied by Nanoindentation and Molecular Dynamics, *Chem. Mater. 2019*, **31**, 1391−1402.

[16] X. Chen, D. Zhang, Y. He, M. U. Ali, Y. Wu, C. Zhao, P. Wu, C. Yan, F. Wudl and H. Meng, Fluoro-alkyl Substituted Isothianaphthene Bisimides as Stable n-Type Semiconductors, *Mater. Chem. Front*., 2020, https://doi.org/10.1039/D0QM00137F.

[17] Byung Jun Jung, Jia Sun, Taegweon Lee, Amy Sarjeant, and Howard E. Katz, Low-Temperature-Processible, Transparent, and Air-Operable n-Channel Fluorinated Phenylethylated Naphthalenetetracarboxylic Diimide Semiconductors Applied to Flexible Transistors, *Chem. Mater*. 2009, **21***,* 94–101.

[18] Brooks A. Jones, Michael J. Ahrens, Myung-Han Yoon, Antonio Facchetti, Tobin J. Marks, and Michael R. Wasielewski, High-Mobility Air-Stable n-Type Semiconductors with Processing Versatility: Dicyanoperylene- 3,4:9,10-bis(dicarboximides), *Angew. Chem. Int. Ed.* 2004, **43**, 6363 –6366.